NASA TECHNICAL NOTE

NASA TN D-2613

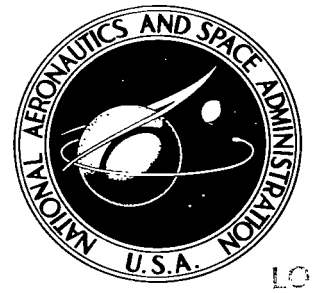

NASA TN D-2613

RESIDUAL STRENGTH OF ALLOYS POTENTIALLY USEFUL IN SUPERSONIC AIRCRAFT

by I. E. Figge

Langley Research Center
Langley Station, Hampton, Va.

NATIONAL AERONAUTICS AND SPACE ADMINISTRATION • WASHINGTON, D. C. • FEBRUARY 1965

RESIDUAL STRENGTH OF ALLOYS POTENTIALLY USEFUL IN SUPERSONIC AIRCRAFT

By I. E. Figge

Langley Research Center
Langley Station, Hampton, Va.

NATIONAL AERONAUTICS AND SPACE ADMINISTRATION

For sale by the Office of Technical Services, Department of Commerce,
Washington, D.C. 20230 -- Price $2.00

RESIDUAL STRENGTH OF ALLOYS POTENTIALLY USEFUL IN SUPERSONIC AIRCRAFT

By I. E. Figge
Langley Research Center

SUMMARY

Residual static-strength tests were conducted on sheet specimens 8 inches (20 cm) wide containing central fatigue cracks of various lengths. Included in this investigation were several stainless-steel and aluminum alloys, one titanium alloy at two thicknesses, and one nickel-base alloy. Tests were conducted at -109° F (195° K), 80° F (300° K), and 250° F (394° K) for the aluminum alloys; the remaining alloys were tested at -109° F (195° K), 80° F (300° K), and 550° F (561° K). The 0.050-inch (1.27-mm) thick Ti-8Al-1Mo-1V (duplex annealed) demonstrated the most favorable overall residual static-strength-to-density ratios. Of the aluminum alloys the clad RR-58 demonstrated the most favorable ratios. Analysis of the data by the use of the unified notch-strength analysis method of NASA TN D-1259 is discussed. Included are some comments on the effect of heat treatment and thickness on residual static strength of Ti-8Al-1Mo-1V. Slow crack growth data are presented for several alloys.

INTRODUCTION

The information presented herein is from the second part of a study to determine the residual static-strength properties of structural materials suitable for use in supersonic aircraft construction; the first part of the study is reported in reference 1. The materials reported herein include several stainless-steel and aluminum alloys, one titanium alloy at two thicknesses, and one nickel-base alloy. Tests on the aluminum alloys were conducted at temperatures of -109° F (195° K), 80° F (300° K), and 250° F (394° K); the remainder of the alloys were tested at -109° F (195° K), 80° F (300° K), and 550° F (561° K). The range of temperatures assigned to the aluminum alloys approximates the temperature extremes encountered by portions of the primary structures of Mach 2 aircraft, while the latter temperature range pertains to aircraft capable of Mach 3 flight.

Data on slow crack growth were obtained for several materials by using photographic techniques. The effects of annealing condition and heat treatment on the residual strength of Ti-8Al-1Mo-1V were also studied. The experimental results were analyzed by using the unified notch-strength analysis method (refs. 1 and 2).

SYMBOLS

The units used for the physical quantities defined in this paper are given both in the U.S. Customary Units and in the International System of Units (SI). Factors relating the two systems are given in reference 3.

a	half-length of internal crack prior to loading, inches or centimeters (cm)
a_f	half-length of internal crack immediately prior to rapid fracture, inches or centimeters (cm)
E	modulus of elasticity, ksi or giganewton/meter^2 (GN/m^2)
$E_{s,n}$	secant modulus corresponding to net-section stress, ksi or giganewtons/meter^2 (GN/m^2)
$E_{s,p}$	secant modulus corresponding to the peak stress, ksi or giganewtons/meter^2 (GN/m^2)
$E_{s,u}$	secant modulus corresponding to stress at ultimate load, ksi or giganewtons/meter^2 (GN/m^2)
e	elongation in 2-inch (5.08-cm) gage length, percent
K_N	stress-concentration factor corrected for size effect (Neuber factor)
K_{TN}	asymptotic limit of K_N as $\rho \to 0$
K_u	static notch-strength factor
S_n	tensile strength of notched specimen at failure (based on net section before loading starts), ksi or meganewton/meter^2 (MN/m^2)
S_f	tensile strength of notched specimen at failure (based on net section immediately prior to rapid failure), ksi or meganewtons/meters^2 (MN/m^2)
S_i	net section stress of notched specimen at onset of slow crack growth, ksi or meganewtons/meter^2 (MN/m^2)
t	thickness of specimen, inches or centimeters (cm)
w	width of specimen, inches or centimeters (cm)
ρ	notch radius, inches or centimeters (cm)
ρ'	material constant (Neuber Constant), inches or centimeters (cm)

σ_u ultimate tensile strength, ksi or meganewtons/meter^2 (MN/m^2)

σ_y yield strength (0.2-percent offset), ksi or meganewtons/meter^2 (MN/m^2)

MATERIALS AND SPECIMENS

The materials studied in this investigation and the thickness are presented in the following table:

Material	Thickness, t -	
	in.	mm
AM 367	0.050	1.27
AM 350 (CRT)	0.050	1.27
PH 14-8Mo (SRH 950)	0.050	1.27
Inconel 718	0.050	1.27
Ti-8Al-1Mo-1V (duplex annealed)	0.050	1.27
Ti-8Al-1Mo-1V (duplex annealed)	0.250	6.35
2020-T6	0.050	1.27
2024-T81 (clad)	0.063	1.61
RR-58 (clad)	0.063	1.61
6061-T4	0.050	1.27

The 6061-T4 alloy is not considered a candidate material for use at elevated temperatures. Tests were conducted on this alloy only at 80° F (300° K) to check the agreement with the data reported in reference 2.

For each specific alloy of a given thickness, all material used in this investigation was obtained from the same mill heat. Subsequent heat treating was done at the Langley Research Center on PH 14-8Mo, AM 367, and Inconel 718. The remainder of the material was tested in the as-received condition. Details of the heat treatments and chemical compositions are presented in table I. All phases of heat treating, machining, and handling followed rigid quality control specifications established at Langley. The tensile properties of the materials tested were obtained from standard ASTM tensile specimens and are given in table II. Each result quoted in table II is the average of at least two tests.

The specimen configuration used in the residual static-strength tests is shown in figure 1. Sheet specimens 8 inches (20 cm) wide and 24 inches (61 cm) long were used. The grain direction was parallel to the direction of loading. A crack starter in the form of a slit 0.10 inch (0.25 cm) long and 0.01 inch (0.025 cm) wide was cut by a spark-discharge technique in the center of each specimen perpendicular to the direction of loading.

A crack-propagation investigation (not presented in this paper) was conducted on the specimens prior to the determination of the residual static

strength. Cracks were grown at various stress levels for the crack-propagation study at temperatures of -109° F (195° K), 80° F (300° K), and either 250° F (394° K) for the aluminum alloys or 550° F (561° K) for the remainder of the alloys until they were within approximately 0.2 inch (0.51 cm) of the desired length for the static tests. The nominal net-section-stress ranges used to prepare the specimens for the residual static-strength study were then adjusted as follows: 0 to 15 ksi (104 MN/m^2) for the aluminum alloys, 0 to 27 ksi (186 MN/m^2) for the titanium alloy, and 0 to 40 ksi (276 MN/m^2) for the stainless steels and the nickel-base alloy. The cracks were grown at these new stress levels at 80° F (300° K) until the desired crack lengths were obtained. This procedure was followed to produce a consistent influence of prior stress on the material immediately ahead of the crack tip. Each specimen was then tested statically at the temperature assigned in the crack-propagation investigation.

EQUIPMENT AND TEST PROCEDURE

A 120,000-pound (534 KN) capacity hydraulic jack and a 1,200,000-pound (5340 KN) capacity universal static hydraulic testing machine at the Langley Research Center were used to perform the static tests. A load rate of 30,000 pounds per minute (2225 N/s) was used for all tests. The maximum load at failure was obtained from the load-indicating systems which are an integral part of these testing machines.

During the static tests, all specimens except the 0.25-inch (6.35-mm) thick Ti-8Al-1Mo-1V (duplex annealed) at 80° F (300° K) and two 2024-T81 (clad) specimens were restrained from local buckling in the test section by means of guide plates. The specimens tested at 80° F (room temperature) were clamped between lubricated guides similar to those described in reference 4. A clear plastic window was installed in the guide to facilitate photography of the specimen during the static tests.

Temperatures of -109° F (195° K) were obtained by clamping blocks of dry ice approximately $8 \times 10 \times 1\frac{1}{2}$ in. ($20 \times 25 \times 4$ cm) to each side of the test section. Two blocks with approximately a 1/2-inch (1-cm) space between them were placed on one side of the specimen, one above and one below the crack, to serve as a viewing port. The third block was located on the opposite side in contact with the cracked region. These blocks also served as the guide plates. Thermocouples spotwelded to the specimen and connected to a strip-chart recorder were used to monitor the temperature. The specimen temperature was found to be uniform throughout the test section within 2° F (1° K).

Elevated temperatures were obtained by clamping a sandwich consisting of an insulating block, an electrical-resistance ceramic heating slab, and a graphite block to each side of the test section. As in the cryogenic setup, two heating units were used on one side of the specimen to provide a viewing port. A third heating unit was placed on the opposite side of the specimen in contact with the cracked region. The graphite blocks served as the guides in

this case. The specimen temperature was regulated by means of a saturable reactor temperature controller and was found to be uniform throughout the test section within ±5° F (±3° K). The specimens were brought to temperature and held approximately 5 minutes prior to static testing.

In both the cryogenic- and elevated-temperature setups, pressure was applied to the cooling or heating elements by means of a screw-adjusted pressure plate. These plates were adjusted such that uniform specimen temperatures were obtained with a minimum frictional force being applied to the specimen. It is believed that this frictional force had no significant influence on the test results. Details of the cryogenic- and elevated-temperature-test setups can be seen in reference 5.

A 70mm sequence camera operating at 20 frames per second was used to obtain the slow crack growth data. A grid was photographically printed on each specimen to facilitate measurement of the slow crack growth. The grid spacing was 0.05 inch (1.27 mm). Both metallographic and tensile tests revealed that the grid had no detrimental effects on the materials over the temperature range covered in this investigation. Details of the grid can be found in reference 5. The image of a load-indicating device was photographed on each frame of film by using an optical prism. The load-indicating device measured the output from a load cell which was in series with the specimen. The frame in which the crack first started to move was used to determine the load at the onset of slow crack growth. In some cases, it was impossible to determine the exact frame in which crack propagation initiated. This inability was due to two factors, first, the shadowing effect caused by the plastic zone immediately in front of the crack tip produced a dark area which appeared on the film and obscured the crack tip, secondly, in some cases the quality of photograph was such that accurate determination of the end of the crack was impossible. In such instances an engineering judgment was made as to the appropriate frame to use. It is believed that the estimate of the crack length was accurate within a few percent. The final crack length prior to rapid fracture was obtained from the picture frame immediately prior to the one in which the load decreased from its maximum value. In a few instances, the specimen remained together for several frames after a decrease in maximum load was noted, but in general total failure was observed in the frame in which the decrease in load occurred.

RESULTS AND DISCUSSION

A summary plot of the residual static-strength-to-density ratios is presented in figure 2. Individual residual-strength test results are presented in table III and figure 3. The residual strength data were analyzed by using the unified notch-strength analysis method (ref. 2). The curves obtained by using this method and the values of $\sqrt{\rho'}$ used in the analysis are also presented in figure 3. A brief discussion of the analysis method and the agreement between the predictions for the aluminum and titanium alloys and test results is presented. Data on slow crack growth are presented in table III and figure 4. The effects of heat treatment and thickness on the residual strength of Ti-8Al-1Mo-1V are presented in figures 6 and 7, respectively.

Strength-Density Comparisons

The variation of residual-strength-to-density ratios with $2a/w$ for all materials studied is presented in figure 2. The data were normalized by dividing the residual strengths (based on the net section prior to loading) of each material by its respective density. These results are presented for -109° F (195° K), 80° F (300° K), and 550° F (561° K) (250° F (394° K) for the aluminum alloys). The values of residual strength used in this figure were obtained from curves faired through the actual test data. It appears from figure 2 that Ti-8Al-1Mo-1V (duplex annealed), $t = 0.050$ inch (1.27 mm), demonstrated the most favorable overall residual strength-density ratios. The stainless-steel alloy, AM 350 (CRT), had the highest residual strength-to-density ratios at cryogenic and room temperature but had extremely low ratios at the elevated temperature. Including the materials tested in reference 1, the Ti-8Al-1Mo-1V (triplex annealed) appears the most favorable. Of the aluminum alloys tested, the clad RR-58 alloy demonstrated the most favorable properties.

Observations on Individual Materials

The residual strengths of the individual materials are presented in figure 3 as plots of the net section stress at failure (based on net section prior to loading), S_n plotted against $2a/w$ over the temperature range. In all the alloys tested, there was reduction in the ultimate strength with increasing temperature (table II), whereas in most of the alloys there was little change in the residual strength with increasing temperature.

AM 367.- A very distinct crackling sound was noted throughout the period of slow crack growth at room temperature for the AM 367. It is believed this sound was produced by the failure of localized portions of the material immediately ahead of the advancing crack.

AM 350 (CRT).- Test results on AM 350 (20% CRT), $t = 0.024$-inch (0.51 mm), were reported in reference 1. The AM 350 (CRT), $t = 0.05$ inch (1.27 mm), tested in the present report was cold-rolled to a nominal ultimate tensile strength of 225 ksi (1553 MN/m^2). Although the amount of cold rolling required was nominally the same in both cases (20%), the resulting tensile properties were considerably different (table II). The residual strengths also differed considerably (fig. 3(b)). For convenience, the data from reference 1 are approximated by the dashed lines shown in figure 3(b). In reference 1, it was noted that for short cracks the residual strength of the (20% CRT) material was above the ultimate strength at 550° F (561° K). This phenomenon did not occur in the 0.050-inch (1.27-mm) thick (CRT) material.

Inconel 718.- Several cracks between 0.05 inch and 0.10 inch (1.3 and 2.5 mm) long running parallel to the direction of loading were noted in one Inconel 718 specimen while it was being cycled at room temperature in preparation for static testing. These cracks emanated from the corners of the stress raiser and also approximately 0.2 inch (5.1 mm) from the ends of the fatigue crack. The final fatigue crack was 1.03 inch (2.62 cm) long. The specimen was subsequently tested statically at room temperature. These longitudinal cracks

had no apparent effect on the residual strength of the specimen. (See table III.)

Ti-8Al-1Mo-1V (duplex annealed) t = 0.250 inch (6.35 mm).- The mode of failure for the 0.250-inch (6.35-mm) thick Ti-8Al-1Mo-1V (duplex annealed) alloy at 550° F (561° K) was noticeably different than might be expected. The initial crack opened considerably, in some cases approximately 1/4 of an inch (6.4 mm), before any increase in the crack length was observed. In all cases, once the crack started to propagate under static loading, it grew along the direction of the principal shear stress. This phenomenon did not occur at cryogenic or room temperature. At these temperatures the cracks propagated in a direction normal to the load with little opening of the crack observed. The values of residual strength were higher at the elevated temperature than at room temperature. This phenomenon was not observed in the 0.050-inch (1.27-mm) thick Ti-8Al-1Mo-1V (duplex annealed) alloy. A failed Ti-8Al-1Mo-1V (duplex annealed), t = 0.250 (6.35 mm), specimen tested at 550° F (561° K) is shown in figure 5.

2020-T6 and 2024-T81 (clad).- In both the 2020-T6 and 2024-T81 (clad) aluminum alloys the values of residual strength were in general higher at the elevated temperature than at room temperature.

Observations on Slow Crack Growth

Slow crack growth data were obtained over the temperature range for Inconel 718; Ti-8Al-1Mo-1V (duplex annealed), t = 0.050 (1.27 mm); 2020-T6; 2024-T81 (clad); and RR-58 (clad) and are presented in figure 4 and table III. A limited amount of data was also obtained on Ti-8Al-1Mo-1V (duplex annealed), t = 0.250 (6.35 mm), and is presented only in tabular form (table III).

The slow crack growth data are presented as plots of net section stress against 2a/w. Three points are used to represent each test. The lower point (square symbol) represents the stress at which slow crack growth initiated, the middle point (circle) represents the failure stress based on the initial crack length prior to loading, and the upper point (triangle) represents the failure stress based on the crack length immediately prior to rapid fracture. To aid in interpretation, the data from each test are joined by straight lines (these lines do not represent the trend of the slow crack growth).

With the exception of the 2020-T6 aluminum alloy (fig. 4(c)), the alloys studied demonstrated considerable slow crack growth. The test temperature had little effect on the amount of slow crack growth for each material, but it apparently influenced the net section stress required to initiate slow crack growth. No systematic variation between this stress and the test temperature was evident.

Examination of the analytical results indicated that slow crack growth initiated when the peak stress at the tip of the crack reached a value approximately equal to the numerical average of the ultimate strength and yield strength. (See table III.) The peak stress at the tip of a crack is defined

as the product of K_p times the net section stress S_i where

$$K_p = 1 + \left(K_{TN} - 1\right)\frac{E_{s,p}}{E_{s,n}}$$

More information is required to determine the mechanism involved in the initiation of slow crack growth.

Effects of Heat Treatment on Residual Strength of Ti-8Al-1Mo-1V

Results of tests on Ti-8Al-1Mo-1V (mill annealed), t = 0.040 inch (1.02 mm), and triplex annealed, t = 0.050 inch (1.27 mm), were reported in reference 1. These results along with the results on duplex-annealed alloy, t = 0.050 inch (1.27 mm), are presented in figure 6. The curves shown represent fairings through the test data.

At -109° F (195° K) and 80° F (300° K), the triplex-annealed alloy demonstrated the most favorable residual-strength properties. At 550° F (561° K) the mill-annealed alloy appeared best. The largest differences in residual strength occurred at the cryogenic temperature. The differences in residual strength decreased with increasing temperature. From figure 6, it appears the triplex-annealed Ti-8Al-1Mo-1V demonstrated the most favorable residual-strength properties over the temperature range.

Effect of Thickness on Residual Strength of Ti-8Al-1Mo-1V (duplex annealed)

The test results for Ti-8Al-1Mo-1V (duplex annealed), t = 0.050 inch (1.27 mm) and t = 0.250 inch (6.35 mm), are presented in figure 7. The curves shown have been faired through the test data. There appeared to be a significant effect of thickness over the temperature range for this material. The thicker specimen had lower values of residual strength at each temperature. The largest effect of thickness on residual strength occurred at -109° F (195° K). This effect decreased with increasing temperature. It is interesting to note that the numerical differences in ultimate tensile strength at each temperature were approximately equal to the differences in the residual strengths.

Analysis by the Unified Notch-Strength Method

The results obtained from the static tests were analyzed by using the unified notch-strength analysis method (refs. 2 and 6). Details of the calculations used are given in the appendix. The Neuber constants $\sqrt{\rho'}$ required in the calculations have been developed previously for the aluminum alloys (ref. 2) and tentative constants have been developed for the titanium alloys (ref. 6).

For convenience, curves of these values are presented in figures 8 and 9. Complete curves of $\sqrt{\rho'}$ plotted against σ_u have not been developed for the stainless-steel and nickel-base alloys as yet. Due to the large variations in chemistry, heat treatments, cold work, and so forth, used in producing these materials it is unlikely that a single (or several) master curves of $\sqrt{\rho'}$ plotted against σ_u will be developed. It is more probable that each alloy will be characterized by a unique curve. The values of $\sqrt{\rho'}$ used in this investigation for the stainless steels and nickel-base alloy were adjusted in such a way that the theory would give a reasonable fit to the present data.

Application of $\sqrt{\rho'}$ curves for titanium.- Test results of Ti-8Al-1Mo-1V (mill annealed and triplex annealed; ref. 1) suggested that the criterion (i.e., α- or $\alpha\beta$-phase alloys) used to distinguish between the two $\sqrt{\rho'}$ curves for the titanium alloys was questionable. The test results of Ti-8Al-1Mo-1V (duplex annealed) in the present investigation further substantiated this belief. Although Ti-8Al-1Mo-1V is considered an α-phase alloy, use of the $\alpha\beta$-plot of $\sqrt{\rho'}$ against σ_u produced the best agreement with the experimental data over the entire temperature range for the 0.050-inch (1.27-mm) thick material (fig. 3(e)). As noted in reference 1, it appeared that two distinct $\sqrt{\rho'}$ curves are required for the titanium alloys, but the choice of the appropriate curve should not be based solely on the material phase but should also include some additional parameters. At present, not enough data are available to clearly define these parameters.

Agreement between predictions for the aluminum and titanium alloys and test results.- The agreement between the predictions and the test results was excellent for 6061-T6 aluminum alloy (using the complete stress-strain curve) and the 0.050-inch (1.27-mm) thick Ti-8Al-1Mo-1V (duplex annealed) alloy over the temperature range (figs. 3(i) and 3(e)). The predictions were considerably higher than the test results for the 0.250-inch (6.35-mm) thick Ti-8Al-1Mo-1V (duplex annealed) alloy (fig. 3(f)). It is believed this lack of agreement is due to the inadequacy of the analysis method to account for thickness effects. The agreement was also extremely poor for the 2020-T6, clad 2024-T81, and clad RR-58 aluminum alloys (figs. 3(g) to 3(i)). The predictions were higher than the test results for the 2020-T6 alloy and lower than the test results for the clad 2024-T81 and RR-58 alloys. This lack of agreement indicates that the present plot of $\sqrt{\rho'}$ against σ_u is not applicable to all aluminum alloys.

SUMMARY OF RESULTS

Residual static-strength tests were conducted on sheet specimens 8 inches (20 cm) wide containing central fatigue cracks of various lengths at temperatures of -109° F (195° K), 80° F (300° K), and 550° F (561° K) (250° F (394° K) for the aluminum alloys). From these tests the following results were obtained:

1. The 0.050-inch (1.27-mm) thick Ti-8Al-1Mo-1V (duplex annealed) alloy demonstrated the most favorable overall residual-strength-to-density ratios; including test results from NASA TN D-2045, the Ti-8Al-1Mo-1V (triplex annealed) alloy demonstrated the most favorable overall residual-strength-to-density ratios.

2. Of the aluminum alloys tested, the RR-58 (clad) alloy demonstrated the most favorable overall residual-strength-to-density ratios.

3. In all cases, there was a reduction in ultimate tensile strength with increasing temperatures, whereas in most cases, there was little change in the residual strength with increasing temperature. The residual strengths of Ti-8Al-1Mo-1V (duplex annealed), 0.250 inch (6.35 mm) thick; 2020-T6; and 2024-T81 (clad); are higher at 550° F (561° K) (250° F (394° K) for the aluminum alloys) than at 80° F (300° K).

4. Thickness affected both the static ultimate and residual strengths of Ti-8Al-1Mo-1V (duplex annealed); the thicker specimens had the lower strengths. Use of the unified-notch analysis method for the thicker specimens resulted in predictions of residual strength that were considerably higher than the test results.

5. Analytical examination of the slow crack growth data indicated that growth initiated when the peak stress at the tip of the crack reached a value approximately equal to the numerical average of the ultimate and yield strength.

Langley Research Center,
National Aeronautics and Space Administration,
Langley Station, Hampton, Va., November 20, 1964.

APPENDIX

METHOD OF CALCULATION

The following is a brief description of the method used to calculate the residual static strength of a sheet specimen containing a fatigue crack. A detailed description of the analysis method can be found in references 2 and 6.

The theoretical stress concentration factor for a sheet specimen containing a fatigue crack is given by

$$K_{TN} = 1 + 2K_w\sqrt{\frac{a}{\rho'}}$$

where from reference 7

$$K_w = \sqrt{\frac{1 - \frac{2a}{w}}{1 + \frac{2a}{w}}}$$

a is one-half the crack length, w is the specimen width, and $\sqrt{\rho'}$ is the Neuber constant. The theoretical factor K_{TN} is then corrected for plasticity by

$$K_u = 1 + \left(K_{TN} - 1\right)\frac{E_{s,u}}{E_{s,n}}$$

where $E_{s,u}$ is the secant modulus corresponding to the stress at the ultimate load, and $E_{s,n}$ is the secant modulus corresponding to the net-section stress. For net-section stresses below the proportional limit $E_{s,n}$ is by definition equal to Young's modulus E. In the cases where the complete stress-strain curves (up to failure) were not available, the values of $E_{s,u}$ were estimated by

$$E_{s,u} = \frac{E}{1 + \frac{0.8eE}{\sigma_u}}$$

where e is the elongation in a 2-inch gage length, E is the elastic (Young's) modulus, and σ_u is the ultimate tensile strength. Finally, the residual static strength S_n based on the net section existing at start of test, is given by

$$S_n = \frac{\sigma_u}{K_u}$$

REFERENCES

1. Figge, I. E.: Residual Static Strength of Several Titanium and Stainless-Steel Alloys and One Superalloy at -109° F, 70° F, and 550° F. NASA TN D-2045, 1963.

2. Kuhn, Paul; and Figge, I. E.: Unified Notch-Strength Analysis for Wrought Aluminum Alloys. NASA TN D-1259, 1962.

3. Mechtly, E. A.: The International System of Units - Physical Constants and Conversion Factors. NASA SP-7012, 1964.

4. Brueggeman, W. C.; and Mayer, M., Jr.: Guides for Preventing Buckling in Axial Fatigue Tests of Thin Sheet-Metal Specimens. NACA TN 931, 1944.

5. Hudson, C. M.: Fatigue-Crack Propagation in Several Titanium and Stainless-Steel Alloys and One Superalloy. NASA TN D-2331, 1964.

6. Kuhn, Paul: Notch Effects on Fatigue and Static Strength. Paper presented at Symposium on Aeronautical Fatigue sponsored by ICAF and AGARD (Rome, Italy), Apr. 1963.

7. Dixon, J. R.: Stress Distribution Around Edge Slits in a Plate Loaded in Tension - The Effect of Finite Width of Plate. J. Roy. Aeron. Soc. (Tech. Notes), Vol. 66, No. 617, May 1962, pp. 320-322.

8. Weiss, V.; and Sessler, J. G., eds.: Aerospace Structural Metals Handbook. Volume II - Non-Ferrous Alloys. ASD-TDR-63-741, Vol. II, U.S. Air Force, Mar. 1963.

TABLE I.- HEAT TREATMENT AND CHEMICAL COMPOSITION OF ALLOYS

(a) Material heat treatments

Material	Condition	Thickness		Heat treatment
		in.	mm	
AM 367[1]	----------	0.050	1.27	Annealed 1400° F (1033° K), quench to -100° F (200° K) for 16 hr, aged 8 hr at 850° F (727° K), air cool
AM 350	CRT	.050	1.27	20% cold rolled, tempered 3 to 5 min at 930° F (772° K), air cool
PH14-8Mo[1]	SRH 950	.050	1.27	1700° F (1200° K) for 60 min, air cool, within 1 hr cool to -100° F (200° K), hold 8 hr, 950° F (783° K) for 60 min, air cool
Inconel 718[1]	----------	.050	1.27	Annealed 1325° F (993° K) for 8 hr, furnace cool 20° F/hr (266° K/hr) to 1150° F (894° K), air cool
Ti-8Al-1Mo-1V	Duplex annealed	.050	1.27	1450° F (1061° K) for 8 hr, furnace cool, 1450° F (1061° K) for 15 min, air cool
		.250	6.35	
2020	T6	.050	1.27	See X2020 in reference 8
2024 (clad)	T81	.063	1.61	See reference 8
RR-58 (clad)	Fully heat treated to specification DTD 5070 A	.063	1.61	5 min to 1 hr at 525° C to 530° C (798° K to 803° K) depending on gage, quench in cold water, 10 to 30 hr at 190° C ± 5° C (463° K ± 5° K)
6061	T4	.050	1.27	See reference 8

[1]Heat treated at Langley.

TABLE I.- HEAT TREATMENT AND CHEMICAL COMPOSITION OF ALLOYS - Concluded

(b) Chemical composition

Element	AM 367, percent	AM 350 (CRT), percent		PH 14-8Mo (SRH 950), percent		Inconel 718, percent		Ti-8Al-1Mo-1V (duplex annealed), percent		2020-T6, percent		2024-T81, percent		RR-58 (clad) (DTD 5070A), percent	6061-T4, percent	
		Min.	Max.	Min.	Max.	Min.	Max.	Min.	Max.	Min.	Max.	Min.	Max.		Min.	Max.
C	0.021	0.08	0.12	0.02	0.05		0.10		0.08							
Mn	0.024	0.50	1.25		1.00		0.50			0.30	0.80	0.30	0.90			0.15
P	0.002		0.040		0.015											
S	0.009		0.030		0.015											
Si	0.08		0.50		1.0		0.75				0.40		0.50		0.40	0.80
Ni	3.40	4.00	5.00	7.50	9.50	50.0	55.0							1.2		
CR	14.25	16.00	17.00	13.50	15.50	17.0	21.0						0.10		0.15	0.35
Mo	1.99	2.50	3.25	2.00	3.00	2.80	3.30	0.75	1.25							
Al	0.03			0.75	1.50	0.20	1.00	7.50	8.50	Balance		Balance		Balance	Balance	
Ti	0.35					0.30	1.30	Balance			0.10			0.10		0.15
Fe	Balance	Balance		Balance		Balance			0.30		0.40		0.50	1.0		0.7
Co	15.44															
Cb + Ta						4.50	5.75									
N		0.07	0.13						0.05							
H									0.015							
V								0.75	1.25							
Cu										4.0	5.0	3.8	4.9	2.5	0.15	0.40
Li										0.9	1.7					
Zn											0.25		0.25			0.25
Cd										0.10	0.35					
Mg											0.03	1.2	1.8	1.5	0.8	1.2

TABLE II.- AVERAGE TENSILE PROPERTIES OF MATERIALS TESTED

[Grain direction longitudinal]

Temperature		σ_u		σ_y		E		e, percent 2-in. (5.08-cm) gage	Number of tests
°F	°K	ksi	MN/m^2	ksi	MN/m^2	ksi	GN/m^2		
AM 367									
-109	195	266.0	1835	263.7	1820	31.4×10^3	217	5.0	3
80	300	243.4	1680	242.0	1670	30.7	212	4.2	3
550	561	206.1	1422	201.3	1389	20.1	139	3.8	3
AM 350 (CRT); t = 0.050 in. (1.27 mm)									
-109	195	266.3	1838	222.0	1532	28.6×10^3	197	20.7	3
80	300	223.4	1542	217.5	1501	27.8	192	16.2	3
550	561	197.8	1365	184.5	1273	22.5	155	3.0	3
AM 350 (20% CRT); t = 0.024 in. (0.51 mm); data from ref. 1									
-109	195	251.4	1735	175.2	1209	28.9×10^3	199	19.0	5
80	300	204.5	1411	182.3	1258	28.6	197	18.8	5
550	561	158.3	1092	154.7	1067	27.9	193	2.7	4
PH 14-8Mo (SRH 950)									
-109	195	272.8	1882	234.4	1617	29.4×10^3	203	13.4	5
80	300	243.3	1679	209.0	1442	28.7	198	8.7	3
550	561	202.3	1396	174.5	1204	23.3	161	8.5	3
Inconel 718									
-109	195	195.0	1346	161.2	1112	27.8×10^3	192	28.0	3
80	300	193.7	1337	162.2	1119	27.8	192	23.3	3
550	561	172.1	1187	144.7	998	26.8	185	19.0	4
Ti-8Al-1Mo-1V (duplex annealed); t = 0.050 in. (1.27 mm)									
-109	195	178.0	1228	162.7	1123	17.7×10^3	121	15.3	3
80	300	152.0	1049	133.6	922	18.3	126	12.5	3
550	561	115.5	797	93.7	647	14.1	97	12.0	3
Ti-8Al-1Mo-1V (duplex annealed); t = 0.250 in. (6.35 mm)									
-109	195	157.5	1087	145.6	1005	16.9×10^3	117	11.0	3
80	300	137.4	948	120.0	828	14.8	102	17.3	3
550	561	113.8	785	85.8	592	13.3	92	16.5	2
2020-T6									
-109	195	88.3	609	82.4	569	12.4×10^3	86	7.7	3
80	300	81.8	564	77.5	535	11.3	78	8.8	4
250	394	68.8	475	64.0	442	9.7	67	9.0	3
2024-T81 (clad)									
-109	195	69.0	476	62.2	429	8.8×10^3	61	7.0	3
80	300	63.2	436	57.6	397	9.5	66	7.2	3
250	394	59.3	409	53.3	368	8.4	58	7.5	3
RR-58 (clad)									
-109	195	64.4	445	58.8	406	10.4×10^3	72	8.3	3
80	300	59.2	408	54.6	377	10.0	69	7.0	3
250	394	54.0	373	51.3	354	10.5	72	7.3	3
6061-T6									
80	300	38.1	263	23.3	161	10.0×10^3	69	22.2	2

TABLE III.- RESIDUAL-STRENGTH TEST RESULTS

Temperature		$\frac{2a}{w}$	S_n based on $\frac{2a}{w}$	
°F	°K		ksi	MN/m²
AM 367				
-109	195	0.131	75.8	523
-109	195	.192	109.8	758
-109	195	.561	65.0	449
80	300	.164	166.9	1152
80	300	.500	133.0	918
550	561	.128	127.0	876
550	561	.188	121.4	838
550	561	.511	112.0	773
PH 14-8Mo (SRH 950)				
-109	195	0.133	163.5	1128
-109	195	.249	147.2	1016
-109	195	.375	132.0	911
-109	195	.530	134.9	931
-109	195	.619	146.0	1007
80	300	.124	186.0	1283
80	300	.249	161.6	1115
80	300	.376	144.0	994
80	300	.495	160.2	1105
80	300	.620	151.0	1042
550	561	.124	152.5	1052
550	561	.245	142.4	983
550	561	.377	136.0	938
550	561	.500	129.0	890
550	561	.613	132.3	913

Temperature		$\frac{2a}{w}$	S_n based on $\frac{2a}{w}$	
°F	°K		ksi	MN/m²
6061-T4				
80	300	0.031	29.2	201
80	300	.059	28.3	195
80	300	.128	28.3	195
80	300	.185	27.7	191
80	300	.244	28.8	199
80	300	.375	27.8	192
80	300	.501	27.9	193
80	300	.625	27.6	190
80	300	.750	29.9	206
AM 350 (CRT); t = 0.050 in. (1.27 mm)				
-109	195	0.065	211.9	1462
-109	195	.129	199.0	1373
-109	195	.175	199.5	1377
-109	195	.254	183.9	1269
-109	195	.373	184.3	1272
-109	195	.510	178.0	1228
-109	195	.632	197.4	1362
80	300	.124	209.0	1442
80	300	.190	203.0	1401
80	300	.238	205.0	1415
80	300	.376	193.3	1334
80	300	.533	191.6	1322
80	300	.595	182.0	1256
550	561	.029	177.0	1221
550	561	.120	138.4	955
550	561	.219	136.5	942
550	561	.500	111.0	766
550	561	.636	128.9	889

TABLE III.- RESIDUAL-STRENGTH TEST RESULTS - Continued

Temperature		$\frac{2a}{w}$	S_n based on $\frac{2a}{w}$		Stress at start of slow crack growth, S_i		$\frac{2a_f}{w}$	S_f based on $\frac{2a_f}{w}$	
°F	°K		ksi	MN/m²	ksi	MN/m²		ksi	MN/m²
Ti-8Al-1Mo-1V (duplex annealed); t = 0.250 in. (6.35 mm)									
-109	195	0.123	67.0	462	---	---	0.351	90.7	626
-109	195	.139	71.8	495	---	---	.277	85.6	591
-109	195	.192	59.5	411	---	---	.364	75.6	522
-109	195	.200	60.4	417	---	---	.337	73.1	504
-109	195	.246	64.3	444	---	---	-----	-----	----
-109	195	.387	58.0	400	---	---	.488	70.4	486
-109	195	.482	50.4	348	---	---	-----	-----	----
80	300	.138	[a]87.6	604	---	---	-----	-----	----
80	300	.194	[a]83.2	574	---	---	.475	127.5	880
80	300	.231	[a]85.3	589	---	---	.388	106.8	737
80	300	.363	[a]82.8	571	---	---	.511	107.2	740
80	300	.505	[a]73.4	507	---	---	.629	97.6	673
550	561	.100	90.7	626	---	---	.601	204.0	1408
550	561	.186	88.3	609	---	---	-----	-----	----
550	561	.250	89.6	618	---	---	-----	-----	----
550	561	.358	90.0	621	---	---	-----	-----	----
550	561	.487	85.4	589	---	---	-----	-----	----

[a]Unguided.

TABLE III.- RESIDUAL-STRENGTH TEST RESULTS - Concluded

Temperature		$\frac{2a}{w}$	S_n based on $\frac{2a}{w}$		Stress at start of slow crack growth, S_i		$\frac{2a_f}{w}$	S_f based on $\frac{2a_f}{w}$		$\frac{\sigma_u + \sigma_y}{2}$		$K_p S_i$		$\frac{\sigma_u + \sigma_y}{2K_p S_i}$
°F	°K		ksi	MN/m²	ksi	MN/m²		ksi	MN/m²	ksi	MN/m²	ksi	MN/m²	
Inconel 718														
-109	195	0.124	174.0	1201	136.4	941	0.169	180.2	1243	178.1	1229	171.9	1186	1.04
-109	195	.188	171.6	1184	126.9	876	.256	186.2	1285	178.1	1229	170.0	1173	1.05
-109	195	.250	167.3	1154	126.7	874	.319	184.0	1270	178.1	1229	171.0	1180	1.04
-109	195	.374	162.0	1118	119.5	825	.431	174.3	1203	178.1	1229	170.9	1179	1.04
[b]80	300	.129	164.9	1138	156.9	1083	.175	173.5	1197	178.0	1228	186.7	1288	.95
80	300	.188	161.6	1115	148.5	1025	.231	170.5	1176	178.0	1228	182.7	1261	.97
80	300	.188	162.8	1123	151.4	1045	.225	173.1	1194	178.0	1228	184.7	1274	.96
80	300	.249	161.6	1115	146.5	1011	.307	177.3	1223	178.0	1228	183.1	1263	.97
80	300	.391	158.9	1096	134.5	928	.438	175.8	1213	178.0	1228	178.9	1234	.99
80	300	.497	159.6	1101	136.2	940	.538	172.6	1191	178.0	1228	178.4	1231	1.00
550	561	.163	149.9	1034	90.3	623	.202	157.5	1087	158.4	1093	147.2	1016	1.08
550	561	.253	147.5	1018	81.9	565	.300	159.4	1100	158.4	1093	147.4	1017	1.07
550	561	.376	145.8	1006	80.3	554	.438	163.7	1130	158.4	1093	147.8	1020	1.07
550	561	.516	142.5	983	77.6	535	.575	163.6	1129	158.4	1093	147.4	1017	1.07
Ti-8Al-1Mo-1V (duplex annealed); t = 0.050 in. (1.27 mm)														
-109	195	0.125	104.5	721	74.0	511	0.287	129.4	893	170.4	1176	172.0	1187	0.99
-109	195	.190	98.7	681	61.4	424	.374	128.8	889	170.4	1176	170.0	1173	1.00
-109	195	.250	89.9	620	61.3	423	.431	121.4	838	170.4	1176	171.0	1180	1.00
-109	195	.378	89.5	618	50.4	348	.525	122.4	845	170.4	1176	169.3	1168	1.01
-109	195	.503	77.1	532	48.8	337	.619	103.1	711	170.4	1176	169.2	1167	1.01
80	300	.127	117.9	814	86.2	595	.263	142.5	983	142.8	985	145.7	1005	.98
80	300	.188	109.1	753	76.3	526	.381	141.2	974	142.8	985	145.0	1001	.98
80	300	.249	102.8	709	70.3	485	.424	137.5	949	142.8	985	142.7	985	1.00
80	300	.438	92.9	641	48.0	331	.599	132.7	916	142.8	985	138.2	954	1.03
80	300	.626	96.2	664	50.7	350	.713	117.3	809	142.8	985	138.4	955	1.03
550	561	.124	97.7	674	52.2	360	.206	107.1	739	104.6	722	96.1	663	1.09
550	561	.188	95.9	662	39.3	271	.231	101.9	703	104.6	722	94.3	651	1.11
550	561	.250	96.3	664	38.9	268	.313	104.4	720	104.6	722	94.5	652	1.11
550	561	.358	97.1	670	38.8	268	.413	107.6	742	104.6	722	94.7	653	1.10
550	561	.490	91.9	634	45.0	311	.538	106.8	737	104.6	722	95.9	662	1.09
2020-T6														
-109	195	0.253	21.3	147	21.2	146	0.254	21.4	148	85.4	589	84.6	584	1.01
-109	195	.312	19.6	135	19.5	135	.313	19.7	136	85.4	589	84.4	582	1.01
-109	195	.363	16.5	114	-----	------	-----	-----	------	85.4	589	-----	------	----
80	300	.064	38.0	262	11.5	79	.081	40.5	279	79.7	550	77.3	533	1.03
80	300	.126	28.5	197	12.2	84	.150	29.7	205	79.7	550	78.1	539	1.02
80	300	.255	22.6	156	6.7	46	.275	24.4	168	79.7	550	-----	------	----
80	300	.292	22.0	152	9.3	64	.313	22.9	158	79.7	550	77.4	534	1.03
80	300	.433	21.4	148	4.5	31	.437	21.8	150	79.7	550	-----	------	----
250	394	.122	43.9	303	28.7	198	.150	46.6	322	66.4	458	67.7	467	.98
250	394	.260	30.5	210	21.4	148	.281	32.8	226	66.4	458	66.6	460	1.00
250	394	.374	30.7	212	18.8	130	.394	34.8	240	66.4	458	66.2	457	1.00
250	394	.435	31.9	220	14.3	99	.456	-----	------	66.4	458	-----	------	----
2024-T81 (clad)														
-109	195	0.126	47.3	326	-----	------	-----	-----	------	65.6	453	-----	------	----
-109	195	.188	43.7	302	18.3	126	0.281	48.3	333	65.6	453	67.9	469	0.97
-109	195	.238	46.8	323	16.2	112	.319	50.9	351	65.6	453	65.6	453	1.00
-109	195	.286	38.3	264	14.4	99	.444	43.0	297	65.6	453	65.1	449	1.01
-109	195	.499	34.5	238	10.8	75	.588	45.2	312	65.6	453	63.8	440	1.03
80	300	[a].097	51.2	353	-----	------	-----	-----	------	60.4	417	-----	------	----
80	300	.102	53.7	371	27.9	193	.156	59.4	410	60.4	417	62.2	429	.97
80	300	.124	48.7	336	27.1	187	.175	54.4	375	60.4	417	62.3	430	.97
80	300	.188	43.0	297	24.3	167	.263	49.6	342	60.4	417	62.0	428	.97
80	300	.200	43.2	298	27.8	192	.300	51.6	356	60.4	417	63.4	437	.95
80	300	[a].201	47.0	324	-----	------	-----	-----	------	60.4	417	-----	------	----
80	300	.275	38.4	265	-----	------	-----	-----	------	60.4	417	-----	------	----
80	300	.305	39.4	272	22.7	157	.400	42.8	295	60.4	417	62.0	428	.97
80	300	.500	35.5	245	18.6	128	.563	43.5	300	60.4	417	60.8	420	.99
250	394	.124	50.6	349	28.7	198	.181	54.7	377	56.3	388	62.9	434	.90
250	394	.189	47.7	329	23.3	161	.300	58.0	400	56.3	388	58.3	402	.97
250	394	.254	48.8	337	21.7	150	.313	55.6	384	56.3	388	57.9	400	.97
250	394	.341	42.9	296	18.5	128	.413	50.5	348	56.3	388	57.0	393	.99
250	394	.492	41.4	286	18.3	126	.563	45.8	316	56.3	388	57.1	394	.99
RR-58 (clad)														
-109	195	0.179	46.5	320.9	20.9	144.2	0.337	58.6	404.3	61.7	425.7	60.8	419.5	1.02
-109	195	.236	46.2	318.8	22.8	157.3	.407	59.5	410.6	61.7	425.7	61.5	424.4	1.00
-109	195	.344	41.4	285.7	26.5	182.9	.488	55.6	383.6	61.7	425.7	62.6	431.9	.99
-109	195	.362	40.5	279.5	27.2	187.7	.507	54.3	374.7	61.7	425.7	62.8	433.3	.98
-109	195	.554	38.4	265.0	21.7	149.7	.606	42.5	293.3	61.7	425.7	61.8	426.4	1.00
80	300	.064	49.8	343.6	29.7	204.9	.169	57.7	398.1	56.9	392.6	57.5	396.8	.99
80	300	.172	45.5	314.0	29.6		.337	57.3	395.4	56.9		58.2	401.6	.98
80	300	.244	42.7	294.6	-----	------	-----	-----	------	-----	------	-----	------	----
80	300	.303	42.0	289.8	29.2	201.5	.413	50.5	348.5	56.9	392.6	58.3	402.3	.98
80	300	.391	39.7	273.9	24.1	166.3	.581	57.7	398.1	56.9	392.6	57.9	399.5	.98
80	300	.500	41.0	282.9	26.8	184.9	.600	53.1	366.4	56.9	392.6	57.9	399.5	.98
250	394	.190	44.6	307.7	29.7	204.9	.300	53.6	369.8	52.6	362.9	53.1	366.4	.99
250	394	.241	44.0	303.6	28.7	198.0	.356	54.0	372.6	52.6	362.9	52.3	360.9	1.01
250	394	.244	44.2	305.0	25.6	176.6	-----	-----	------	52.6	362.9	53.0	365.7	.99
250	394	.350	42.7	294.6	20.9	144.2	.475	54.3	374.7	52.6	362.9	52.5	362.3	1.00
250	394	.471	40.9	282.2	14.7	101.4	.556	49.1	338.8	52.6	362.9	51.8	357.4	1.02

[a]Unguided.
[b]Specimen a had cracks parallel to direction of loading.

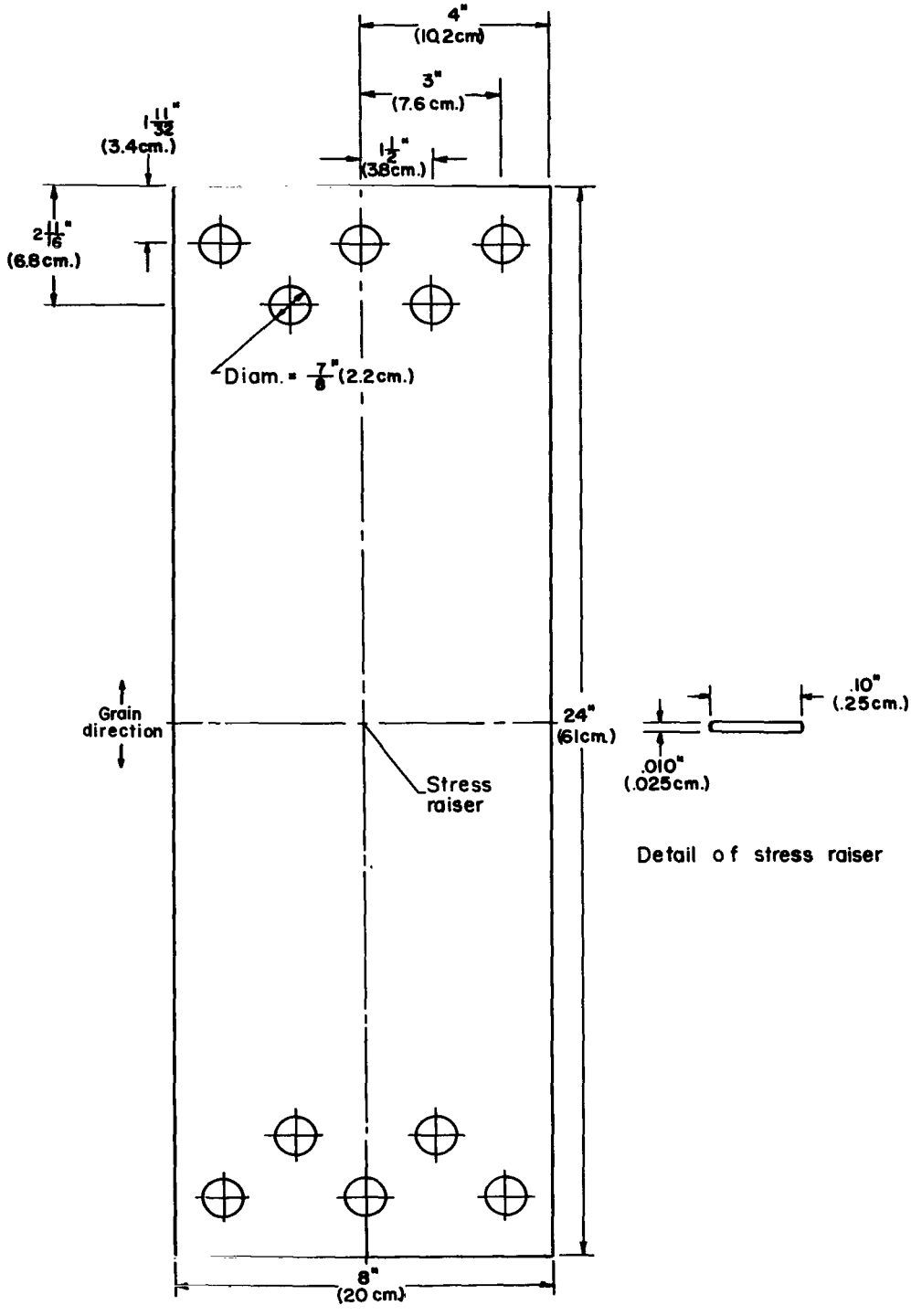

Figure 1.- Specimen configuration.

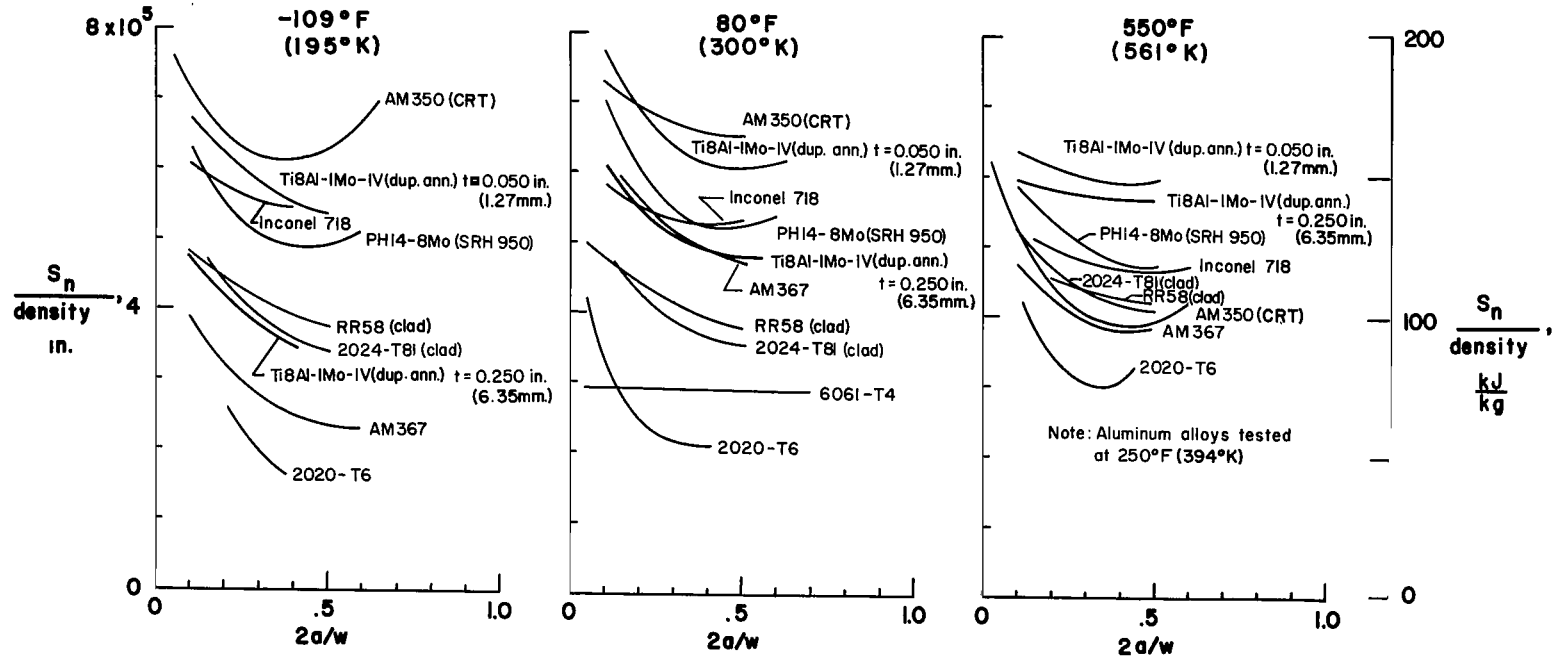

Figure 2.- Variation of residual-strength-to-density ratios with 2a/w. w = 8 in. (20 cm).

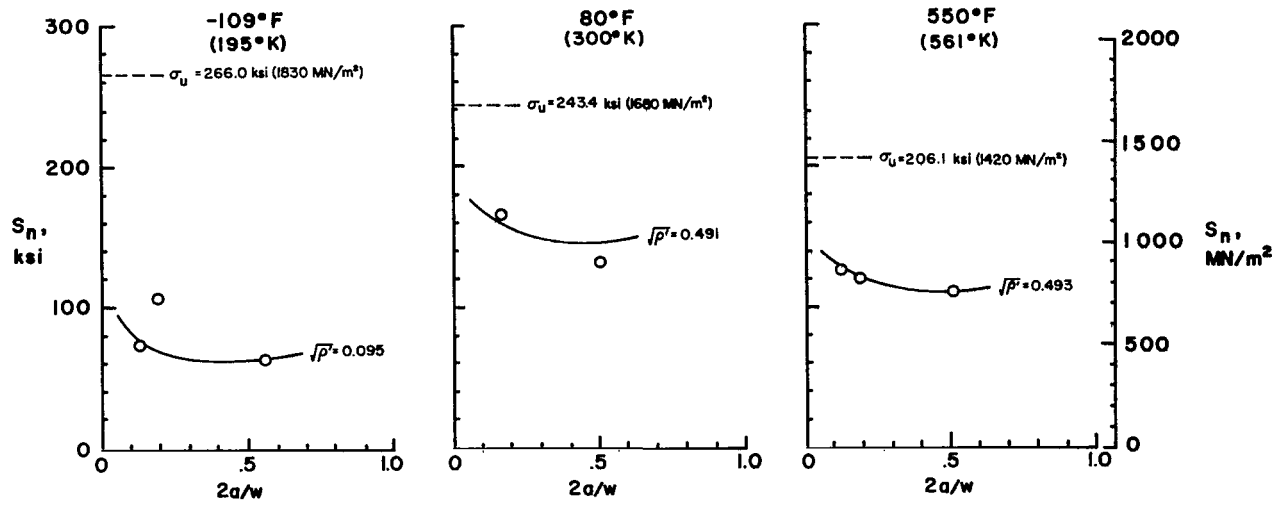

(a) AM 367.

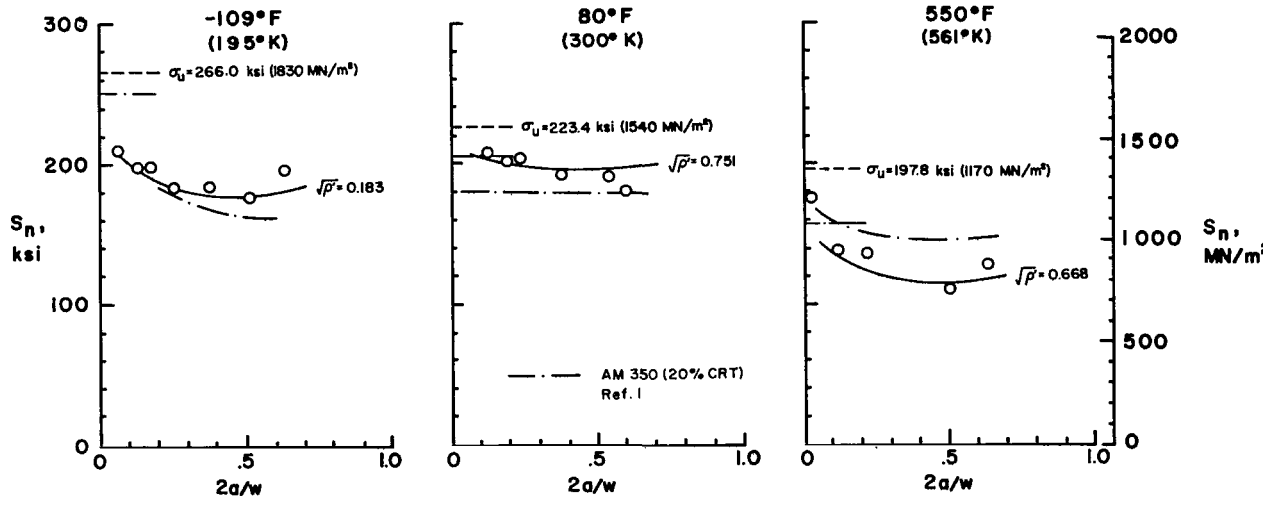

(b) AM 350 (CRT).

Figure 3.- Residual strengths of individual materials. w = 8 in. (20 cm).

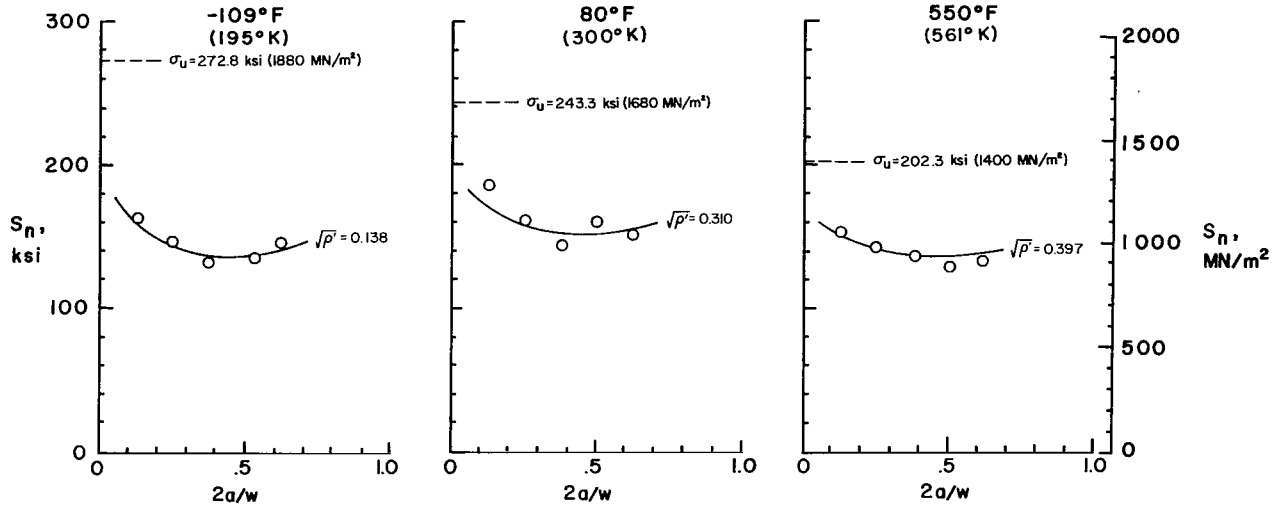

(c) PH 14-8Mo (SRH 950).

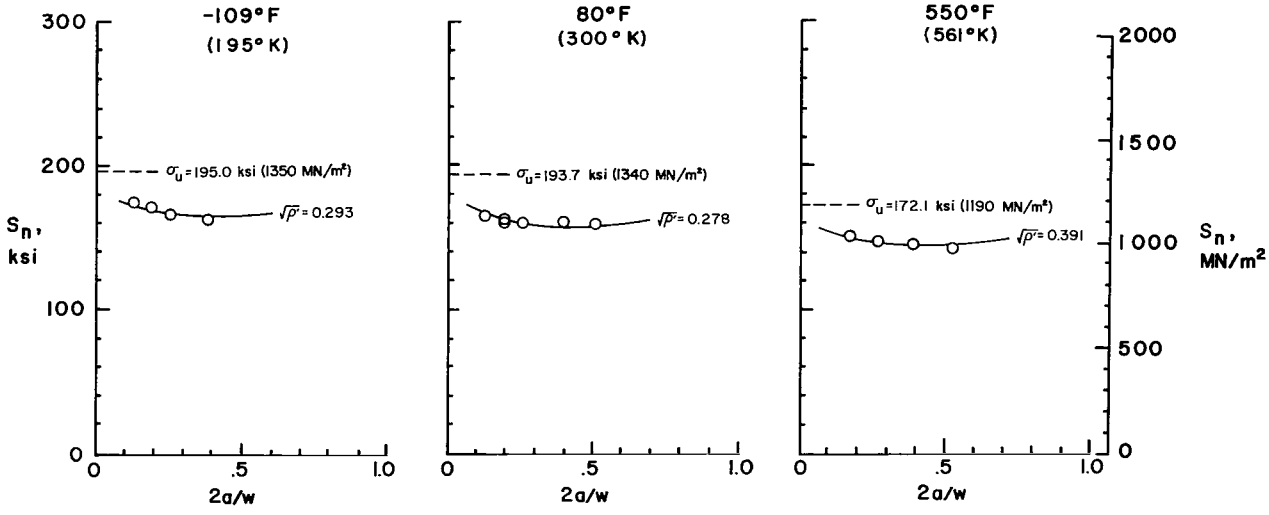

(d) Inconel 718.

Figure 3.- Continued.

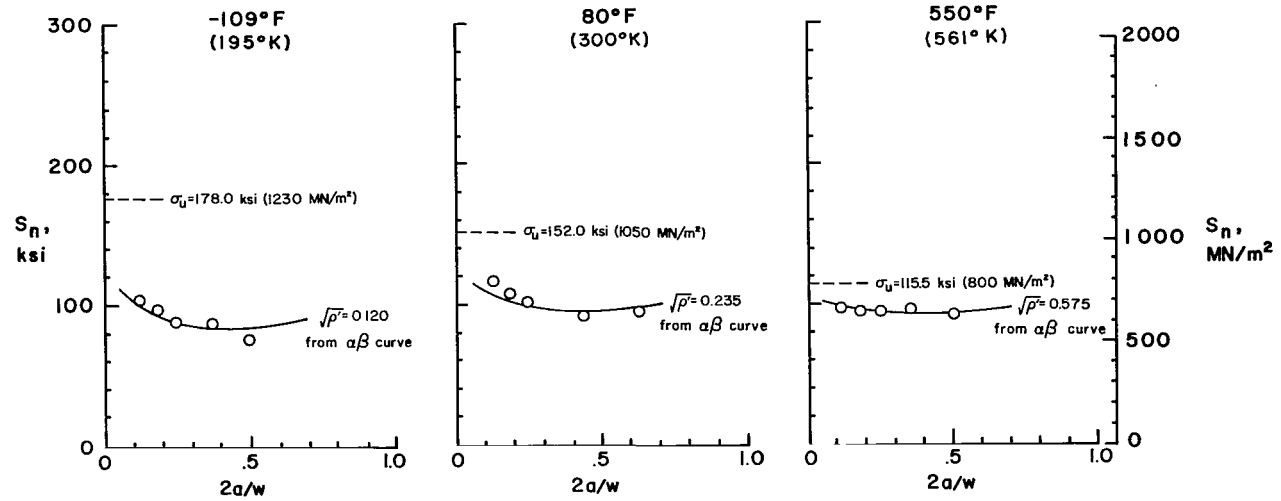

(e) Ti-8Al-1Mo-1V (duplex annealed); t = 0.050 in. (1.27 mm).

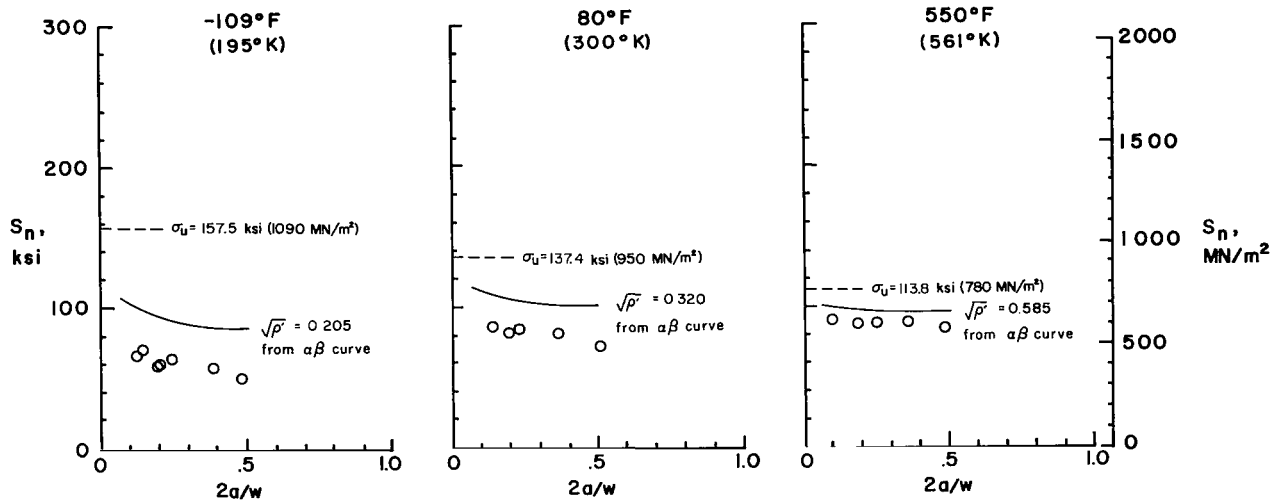

(f) Ti-8Al-1Mo-1V (duplex annealed); t = 0.250 in. (6.35 mm).

Figure 3.- Continued.

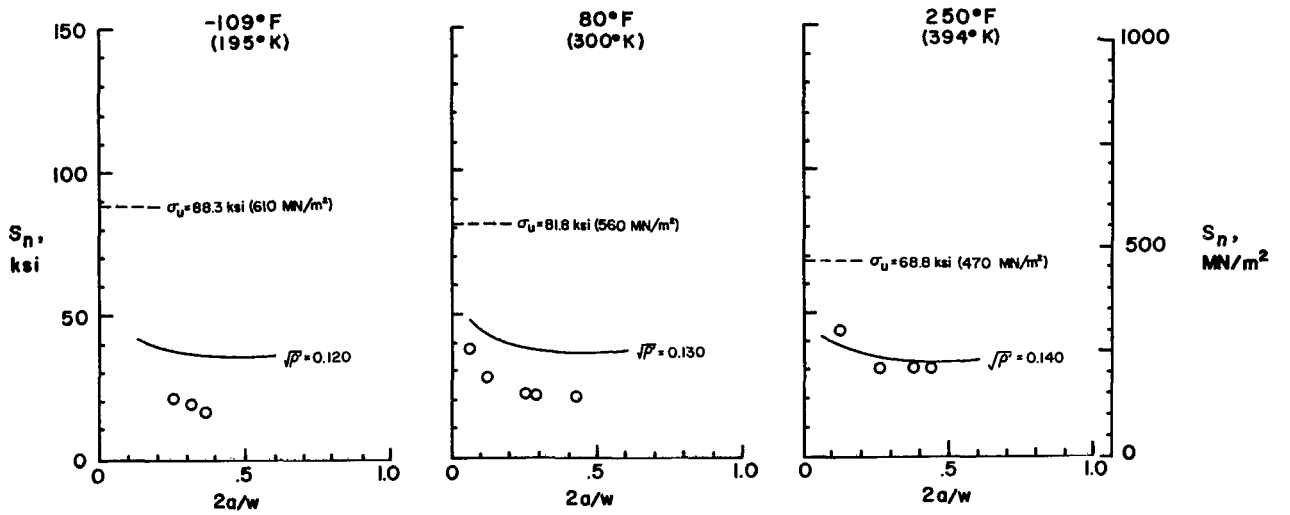

(g) 2020-T6.

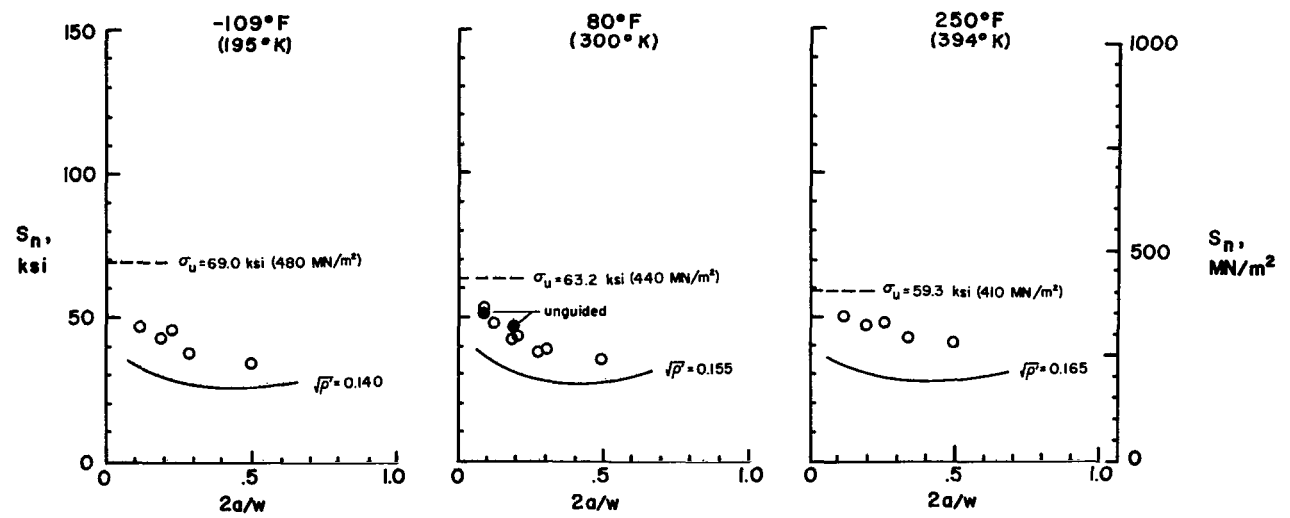

(h) 2024-T81.

Figure 3.- Continued.

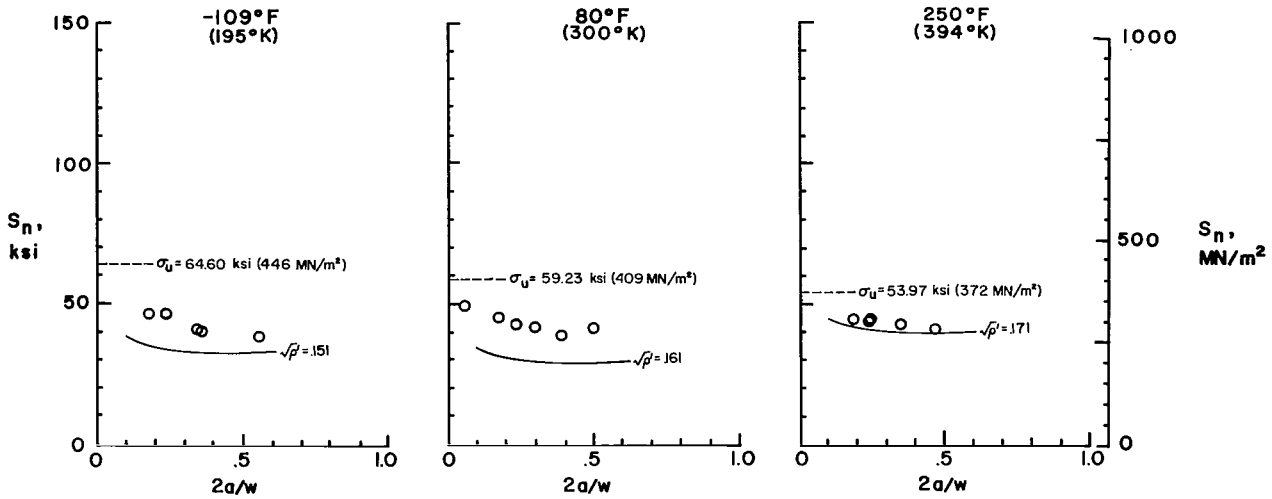

(i) RR-58 (clad).

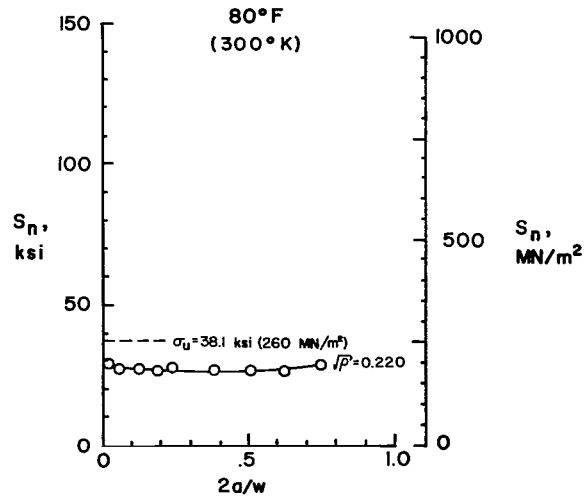

(j) 6061-T4.

Figure 3.- Concluded.

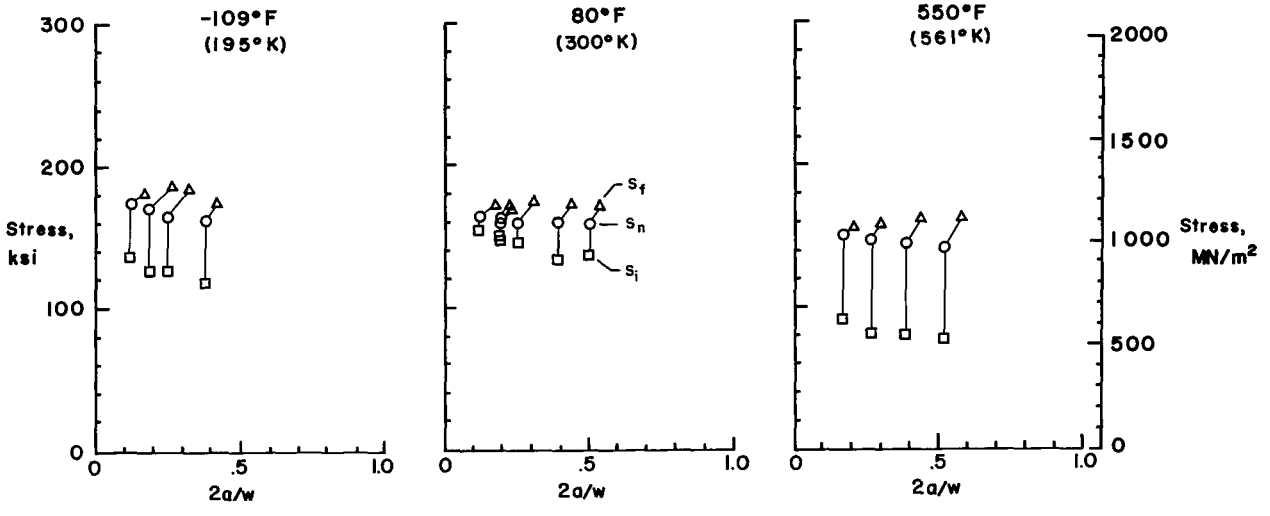

(a) Inconel 718.

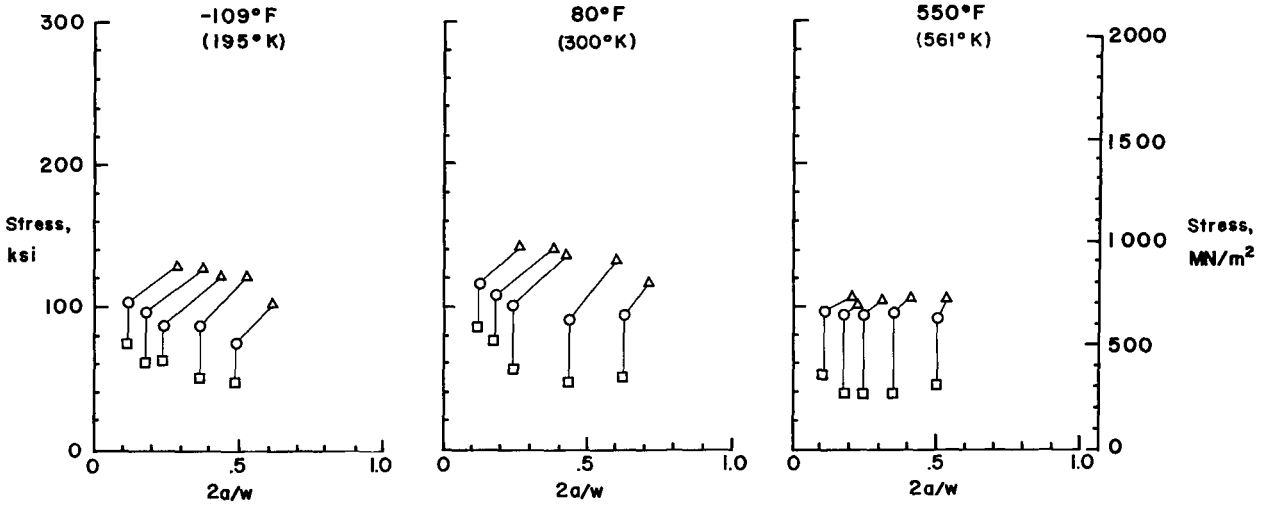

(b) Ti-8Al-1Mo-1V (duplex annealed); t = 0.050 in. (1.27 mm).

Figure 4.- Stress required to initiate slow crack growth and to produce final failure in 8-in. (20-cm) wide sheet specimens.

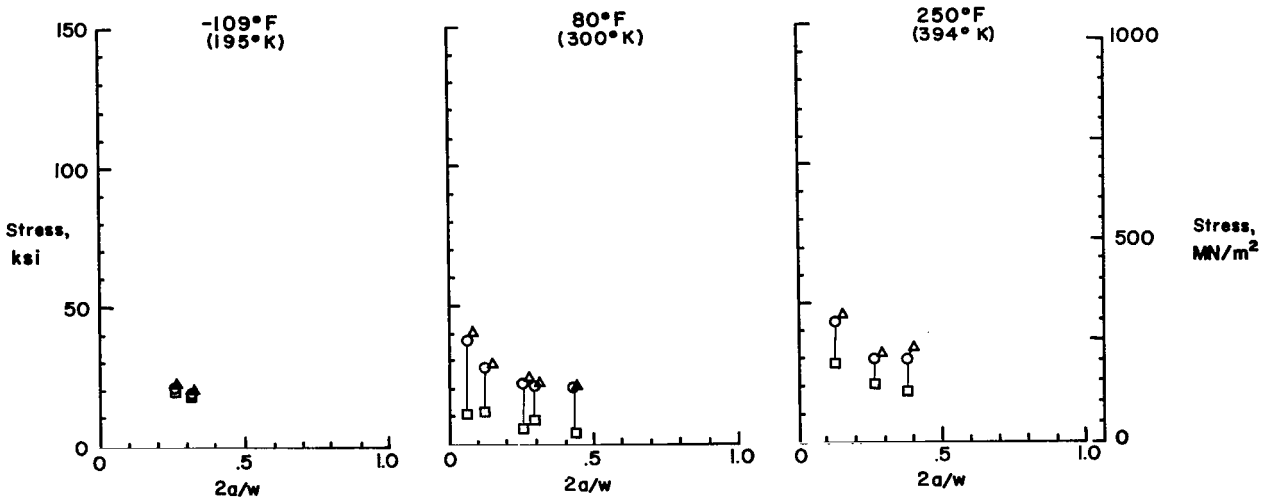

(c) 2020-T6.

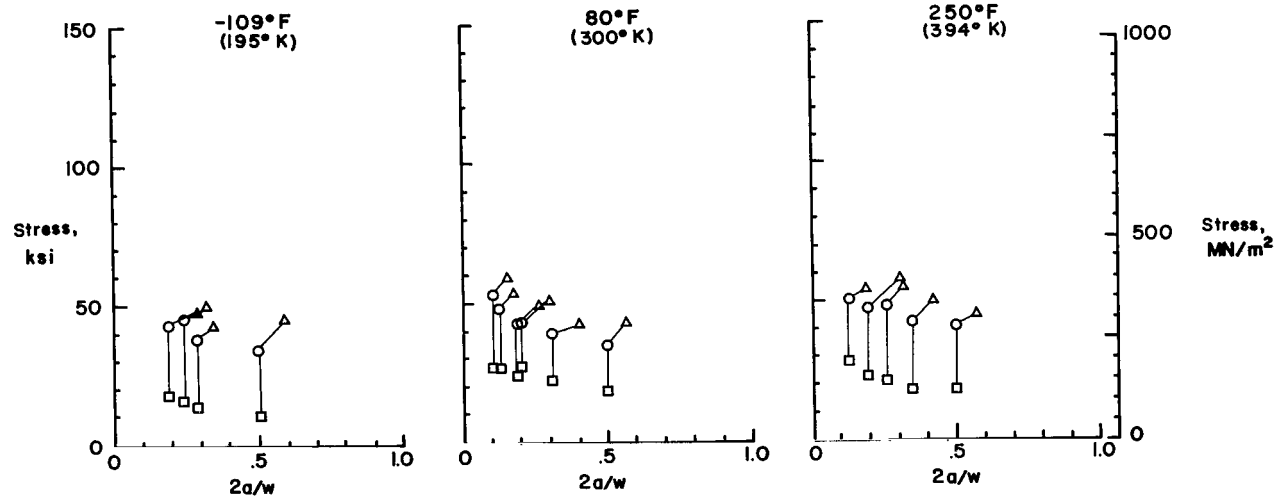

(d) 2024-T81 (clad).

Figure 4.- Continued.

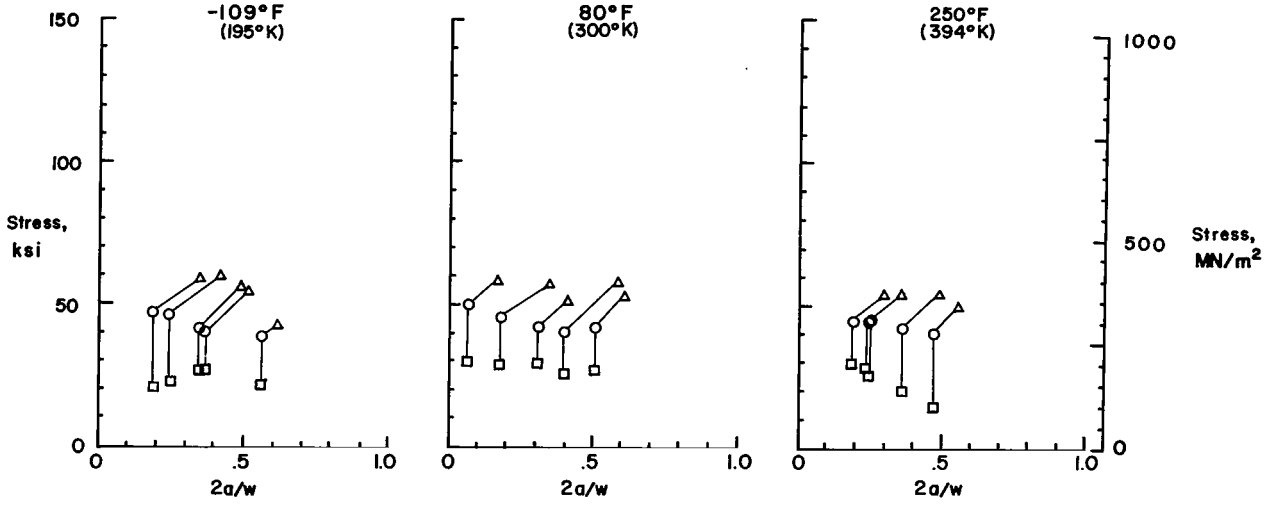

(e) RR-58 (clad).

Figure 4.- Concluded.

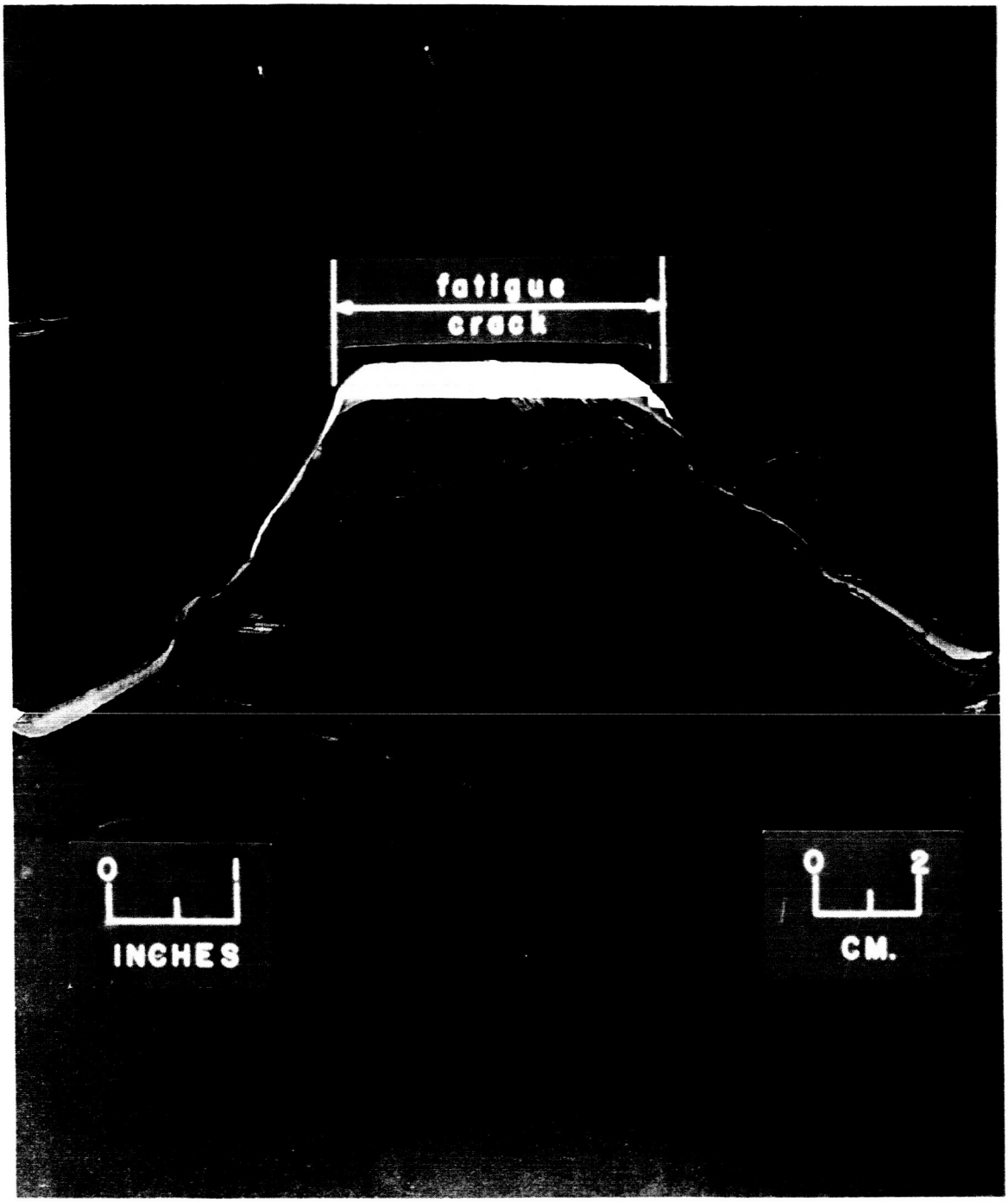

L-64-8006.1

Figure 5.- Failed Ti-8Al-1Mo-1V (duplex annealed), t = 0.250 in. (6.35 mm), specimen tested at 550° F (561° K).

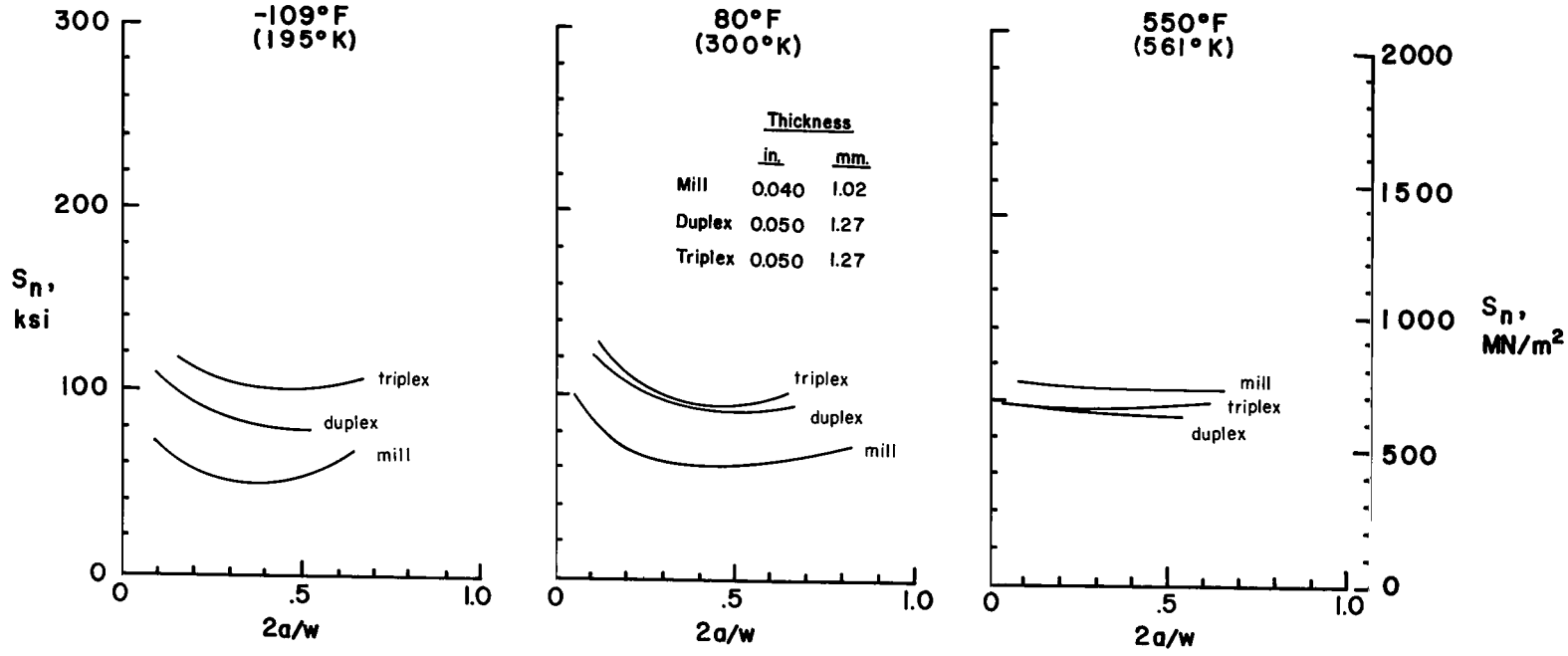

Figure 6.- Effect of annealing condition on residual strength of Ti-8Al-1Mo-1V. w = 8 in. (20 cm).

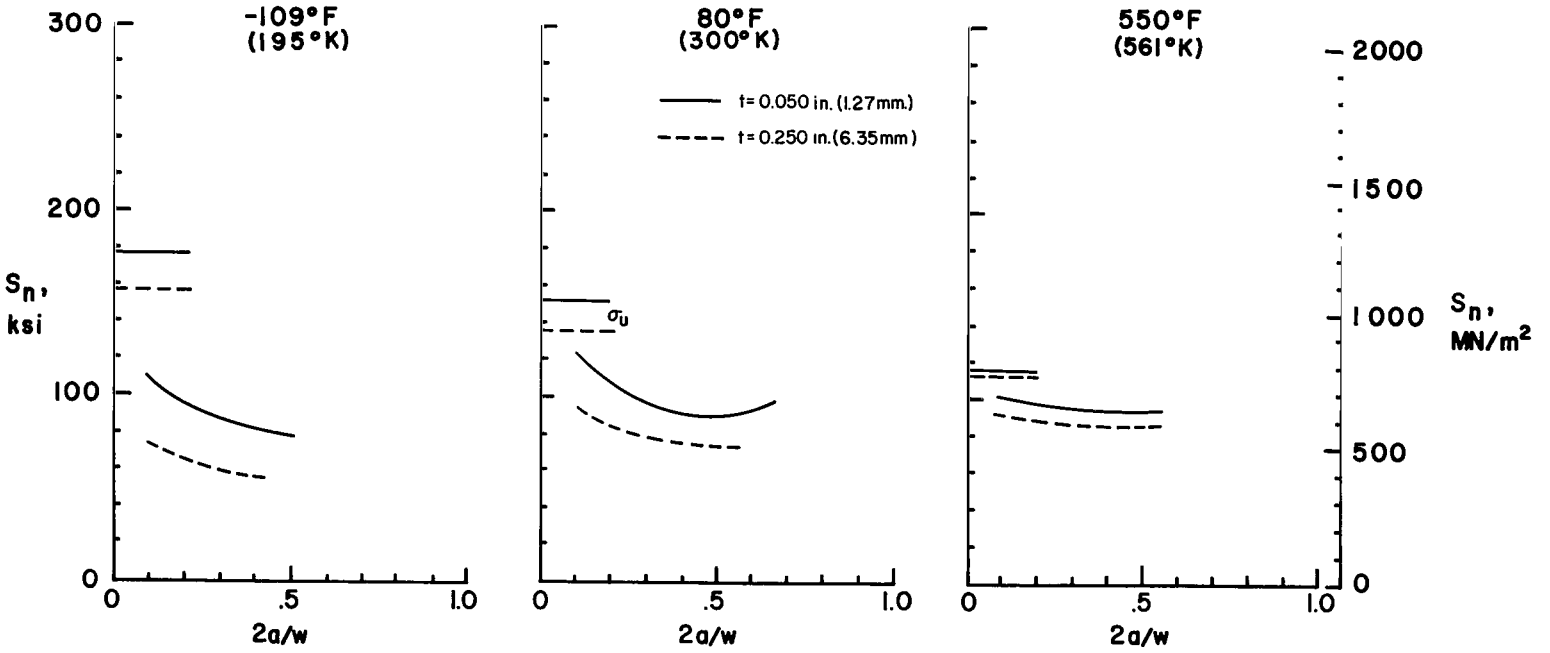

Figure 7.- Effect of thickness on residual strength of Ti-8Al-1Mo-1V (duplex annealed). w = 8 in. (20 cm).

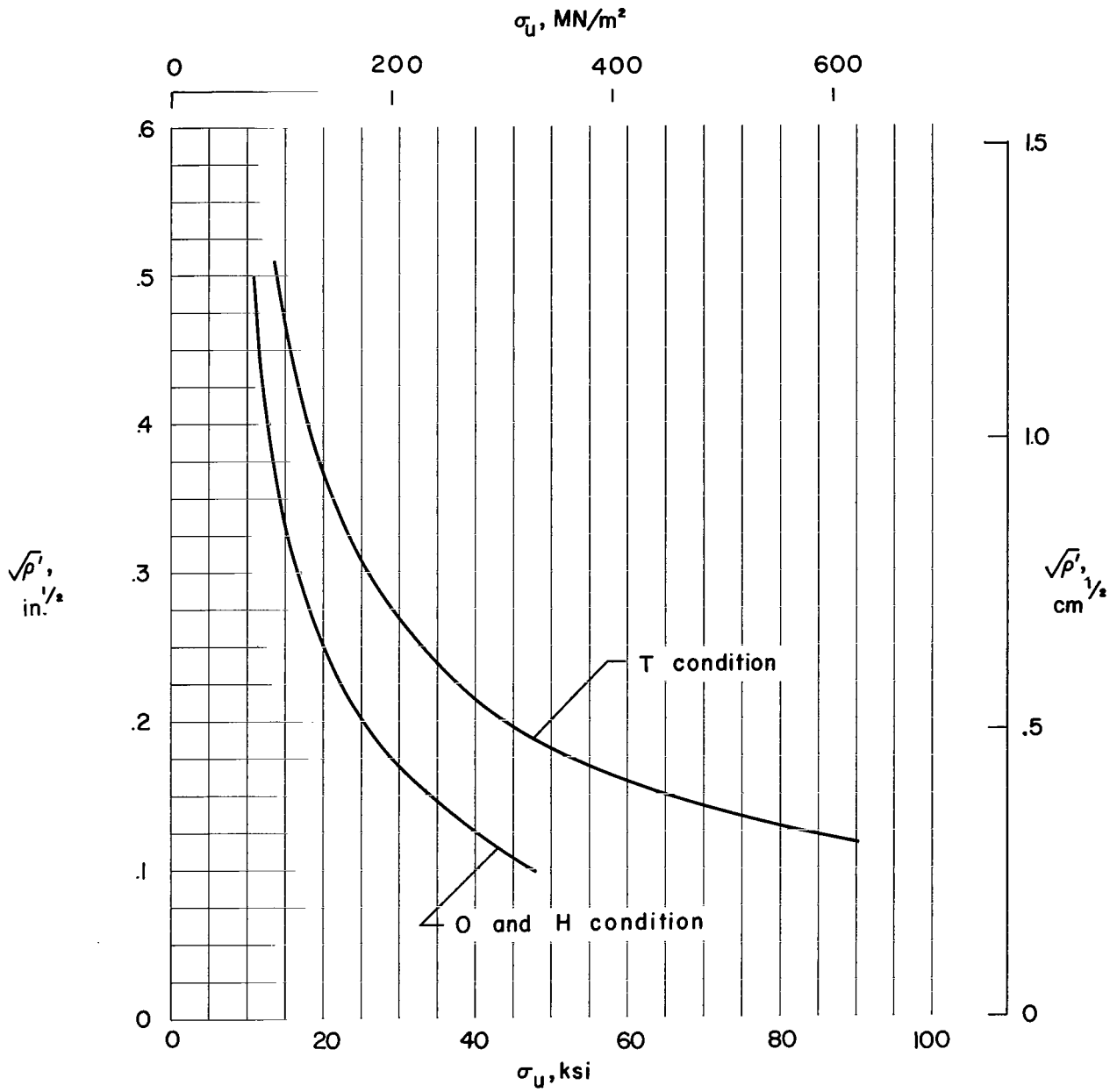

Figure 8.- Neuber constants for wrought aluminum alloys. T, heat treated; O, annealed; H, strain hardened.

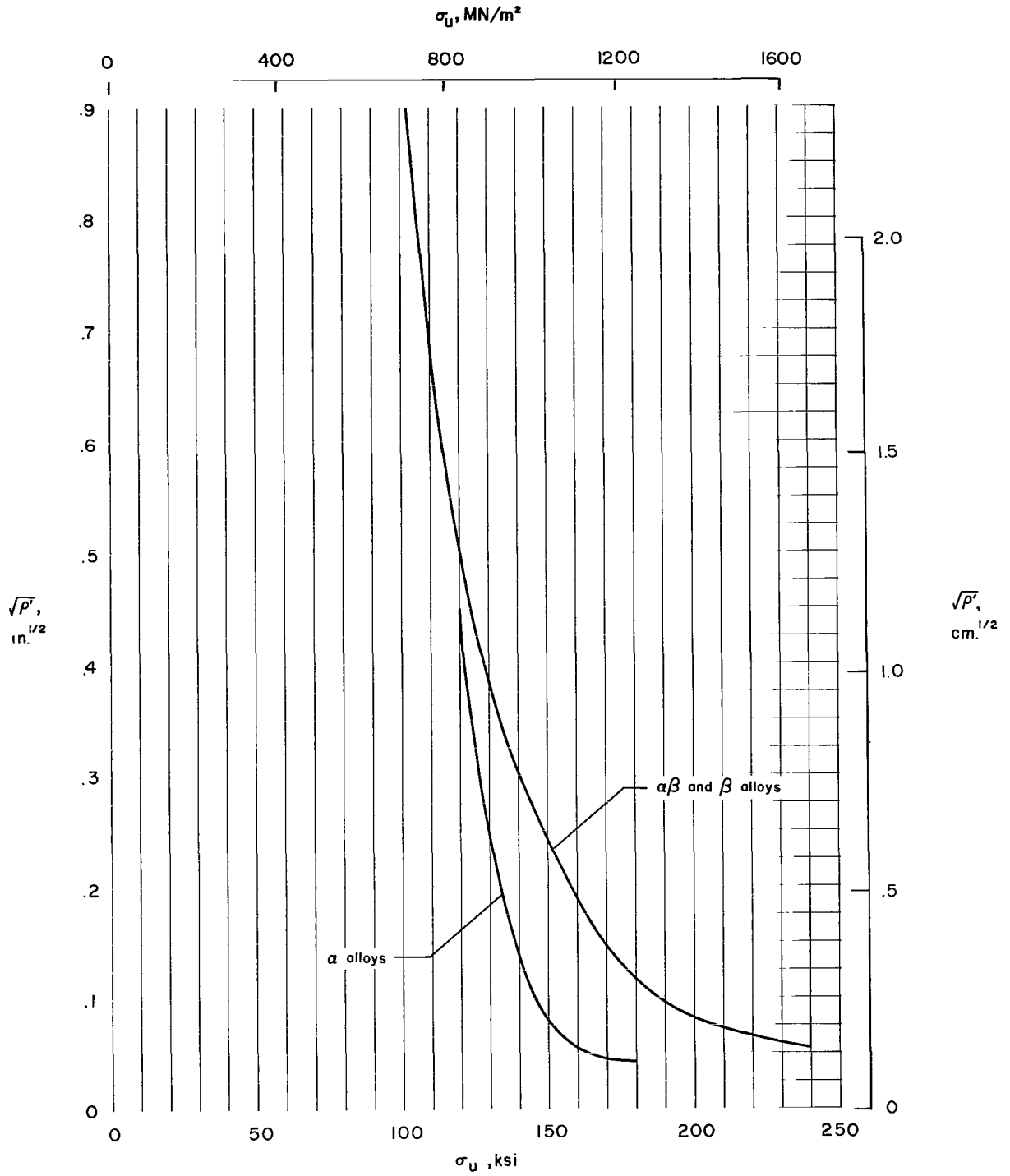

Figure 9.- Tentative Neuber constants for titanium alloys.

"The aeronautical and space activities of the United States shall be conducted so as to contribute . . . to the expansion of human knowledge of phenomena in the atmosphere and space. The Administration shall provide for the widest practicable and appropriate dissemination of information concerning its activities and the results thereof."

—NATIONAL AERONAUTICS AND SPACE ACT OF 1958

NASA SCIENTIFIC AND TECHNICAL PUBLICATIONS

TECHNICAL REPORTS: Scientific and technical information considered important, complete, and a lasting contribution to existing knowledge.

TECHNICAL NOTES: Information less broad in scope but nevertheless of importance as a contribution to existing knowledge.

TECHNICAL MEMORANDUMS: Information receiving limited distribution because of preliminary data, security classification, or other reasons.

CONTRACTOR REPORTS: Technical information generated in connection with a NASA contract or grant and released under NASA auspices.

TECHNICAL TRANSLATIONS: Information published in a foreign language considered to merit NASA distribution in English.

TECHNICAL REPRINTS: Information derived from NASA activities and initially published in the form of journal articles.

SPECIAL PUBLICATIONS: Information derived from or of value to NASA activities but not necessarily reporting the results of individual NASA-programmed scientific efforts. Publications include conference proceedings, monographs, data compilations, handbooks, sourcebooks, and special bibliographies.

Details on the availability of these publications may be obtained from:

SCIENTIFIC AND TECHNICAL INFORMATION DIVISION

NATIONAL AERONAUTICS AND SPACE ADMINISTRATION

Washington, D.C. 20546